



OPEN

The effect of gelatin as pore expander in green synthesis mesoporous silica for methylene blue adsorption

Maria Ulfa¹✉, Didik Prasetyoko², Wega Trisunaryanti³, Hasliza Bahruji⁴, Zahra Ayu Fadila¹ & Novia Amalia Sholeha⁵

Mesoporous silica NSG had been synthesized while employing gelatin as a natural template to successfully increase the particle size and expand the pore diameter of NSG. All silica samples exhibited a similar XRD pattern with a broad peak centred at $2\theta = 22.9^\circ$, as the characteristic of amorphous silica. FTIR results showed that the reduction of Si–O–Si symmetric stretching vibrations at 1075 cm^{-1} was due to the use of a high percentage of gelatin. Moreover, TEM analysis displayed the mesoporous channels in the form of a honeycomb structure with a diameter of $\pm 6\text{ nm}$. Gelatin enhanced the surface area of silica from 467 to $510\text{ m}^2/\text{g}$, the pore volume from 0.64 to 0.72 cc/g and expanded the pore diameter from 3.5 nm to 6.0 nm . The expansion of the ordered mesopores with the increase of P123: gelatin ratios was elucidated by the pore size distribution. The adsorption capacity of methylene blue (MB) was improved on mesoporous silica with an expanded pore dimension to give 168 mg/g adsorption capacity within 70 min .

Mesoporous silica is widely applied as adsorbents for waste removal¹, carrier in drug delivery system², as catalyst supports³ and material for energy storage⁴. Synthesis of silica with high surface area and ordered pore structure is beneficial for a variety of applications as it improves diffusion of molecule reactant. The main concern circumventing the safety of the synthesis procedures is to reduce the use of harmful reagents. Green synthesis aims to minimize the use of synthetic chemicals that are toxic and harmful to the environment^{5,6}. Utilization of biomass waste as silica sources such as rice husk ash and palm residue reduced the reliance on synthetic chemicals^{7,8}. Direct oxidation of silicon-rich biomass waste often produced silica with a low surface area and a non-uniform structure^{7,9} restricting the performance as adsorbent of large molecules such as ibuprofen, dibenzothiophene and methylene blue^{10–12}. The properties of silica obtained from pyrolysis of biomass were improved when the process was combined with acid and alkaline extraction of silica from biomass prior to pyrolysis^{13–16}. However, extraction of silica from fly ash biomass using NaOH only yielded on average of 0.001% of silica from the amount of biomass used¹.

Synthesis of porous material using an environmentally friendly organic–inorganic pore directing agent is also seen as a pathway to suppress the instability of natural material while simultaneously reduce the use of synthetic inorganic materials^{9,11,17}. Tailored synthesis of silica via sol–gel, precipitation, chemical vapour deposition or microemulsion methods produced silica with uniform structures and morphologies^{8,15,18}. The sol–gel method is generally involved the utilization of surfactants or pore-directing molecules in the form of synthetic block copolymers to mould the shape, size and porosity^{1,15}. However, the application of synthetic surfactant is hampered by its expensive price, non-biodegradable properties, and non-sustainable in particular for large-scale production^{15,19,20}. Natural pore-directing molecules from gelatin, gum Arabic and starch have been reported in the synthesis of porous silica^{21–23}. Gelatin is obtained from hydrolysis of animal skin and bone waste which has high sustainability due to the abundant sources and the feasibility of production. The stability of gelatin and

¹Chemistry Education Study Program, Faculty of Teacher Training and Education, Sebelas Maret University, Jl. Ir. Sutami 36A, Surakarta 57126, Indonesia. ²Department of Chemistry, Faculty of Science and Data Analytics, Institut Teknologi Sepuluh Nopember, Keputih, Sukolilo, Surabaya 60111, Indonesia. ³Department of Chemistry, Faculty of Science, Gadjah Mada University, Sekip Utara Sleman, Indonesia. ⁴Centre of Advanced Material and Energy Sciences, University Brunei Darussalam, Jalan Tungku Link 1410, Brunei Darussalam. ⁵College of Vocational Studies, Bogor Agricultural University (IPB University), Jalan Kumpang No. 14, Bogor 16151, Indonesia. ✉email: ulfa.maria2015@gmail.com; mariaulfa@staff.uns.ac.id

Notation of sample	P123: gelatin (w/w)
NS	1:0.00
NSG-1%	1:0.01
NSG-2%	1:0.02
NSG-4%	1:0.04

Table 1. The sample was labelled according to the ratio of P123 and gelatin.

the interaction between the functional group of gelatin and various metal precursor allowed the formation of well-defined crystal structures even after calcination at high temperatures²⁴. Previous research on a hybrid system consisting of synthetic and natural pore-directing molecules was able to produce high surface area carbon microspheres as a result of the combination of gelatin with Pluronic F127⁶. In addition to Pluronic F127, several synthetic templates such as Pluronic P123, CTAB, and CTAOH can control porosity based on their molecular weight, chain length and functional groups^{19,25,26}. These synthetic pore templates have succeeded in producing porous materials such as MCM-41, MCM-48, SBA-15 and KIT^{2,27–29}.

Amine functional groups in gelatin produced electrostatic interaction with silicate ions, capable of directing molecular arrangement for the production of materials with enhanced physicochemical properties^{11,30,31}. In this study, silica nanoparticles with well-defined mesopores were synthesized using gelatin and Pluronic P123 templates. Gelatin is proposed to act as a natural pore directing agent and strengthen the stability of P123 to hold the structure following calcination at high temperatures. This study will observe the effect of gelatin in expanding the pore structure of mesoporous silica. The structural properties of mesoporous silica will be characterized by XRD, FTIR, nitrogen adsorption–desorption and SEM EDX, TEM and its performance will be applied as an adsorbent for methylene blue.

Experimental procedures

Synthesis of mesoporous silica-gelatin (NSG). Surfactant P123 and gelatin were dissolved in concentrated hydrochloric acid (37% v/v) and distilled water then stirred at 500 rpm for 3 h with a temperature of 40 °C. TEOS as a silica source was added and stirred until homogeneous. The molar ratios of the chemicals used in this study were 1 TEOS: 0.017 P123: 5.68 HCl: 197 H₂O. The mixture was continuously stirred at the same temperature for another 24 h. The procedure was repeated with a different ratio of P123: gelatin and labelled as NSG-x%, where x referred to the gelatin concentration given in Table 1.

The mixture was poured into a Teflon line autoclave and heated in an oven for 24 h at 100 °C. The white precipitate obtained was filtered using a Buchner funnel and washed with 200 mL of distilled water. The resulting solid is dried for 24 h at 100 °C and grounded to produce a fine powder. To remove the templates, the solid is calcined at 550 °C for 5 h and placed in a vial at room temperature.

Methylene blue (MB) adsorption. Methylene blue (MB) solution at 50 mg/L was prepared by dissolving methylene blue in deionised water. Then 50 mg of adsorbent was mixed with 200 mL of MB solution and stirred at 200 rpm for 20 min at room temperature. The concentration of MB solution was determined at different contact times by extracting 3 ml of the solution for every 5 min intervals. The effect of adsorbent weight and initial concentration of MB solution were observed using different adsorbent weights (5,10,25, 50, 70 mg) while the initial MB concentration was varied at 10, 20, 50, 100, mg/L. The concentration of MB was determined using UV spectrophotometer (Shimadzu-230PI). The maximum absorption wavelength of methylene blue was recorded at 664 nm. The adsorption capacity of methylene blue on silica sample is calculated using the following equation:

$$q_e = (C_0 - C_e) \frac{w}{m} \quad (1)$$

where C_0 is the initial concentration and C_e is the equilibrium concentration (mg/L) of MB in the bulk phase. The symbol w represents the amount of liquid phase (L) while m is the weight of the adsorbent (g). The adsorption kinetics model was calculated using the Pseudo First Order³² and the Pseudo Second Order as given in Eqs. (2) and (3)³³, respectively.

The Pseudo First Order

$$\ln(q_e - q_t) = \ln q_e - k_1 t \quad (2)$$

The Pseudo Second Order

$$\frac{t}{q_t} = \frac{1}{k_2 q_e^2} + \frac{1}{q_e} t \quad (3)$$

where q_e is adsorption capacity at equilibrium (mg/g), q_t is adsorption capacity at time t (mg/g), k_1 and k_2 as rate constant price/slope (per minute) and t as contact time (minutes).

Characterization of the catalyst. Nitrogen adsorption–desorption analysis was performed on a Quantachrome Autosorb Automated Gas Sorption System, with an outgas temperature of 300 °C and a bath temperature of 77 K. Analysis of the N₂ adsorption data was performed using Autosorb for windows 1.2 provided

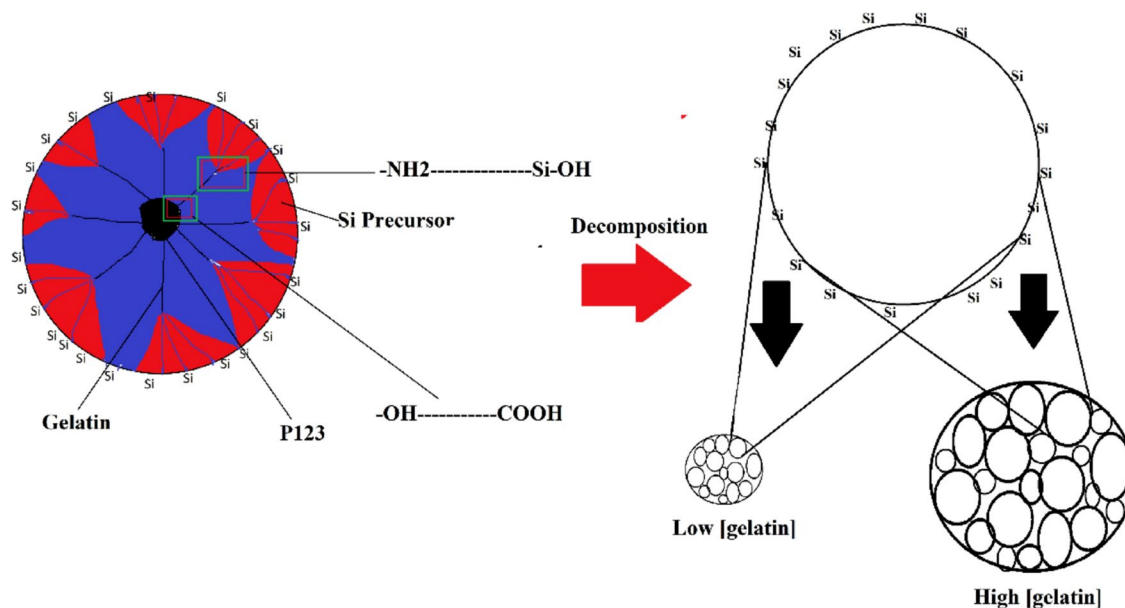


Figure 1. The micellar aggregation from P123-gelatin with Si precursor for NSG formation.

by Quantachrome Co. The surface area was calculated through a multipoint BET model using the P/P_0 ranging from 0.05 to 0.2. The pore size distribution was calculated using a BJH model; and the total pore size was calculated in terms of the maximum P/P_0 point. The crystalline phase was investigated using Philips X'pert XRD instrument with Cu K α radiation with a step size of 0.04° and counting time of 10 s. The data were recorded in the 2-theta range in small angle $0.1\text{--}5.0^\circ$ and wide angle of $5\text{--}80^\circ$. The morphology and element of sample was monitored by the micrograph of Scanning Electron Microscopy (SEM- EDX ZEIS EVO MA 10) and coated by Pd/Au and Transmission Electron Microscopy (TEM HT7700, 120 kV). The analysis of functional group conducted at range $400\text{--}4000\text{ cm}^{-1}$ by Fourier transform infrared spectroscopy (FTIR Shimadzu Spectrometer 2800).

Results and discussion

Mesoporous silica synthesized in the presence of gelatin showed the enlargement of mesopore diameter and particle size originated from the formation of stable micellar network between gelatin and P123 block copolymer (Fig. 1). Tetraethyl orthosilicate as silica source is spontaneously hydrolysed when added in water to form SiO_2 . However, the presence of P123 surfactant, displaced $\text{C}_2\text{H}_5\text{O}^-$ on SiO_4^- with the triblock PEO copolymer preventing the hydrolysis to SiO_2 . The presence of gelatin further stabilised the PEO structure via interaction between the --COO^- fragments in gelatin with --OH in PEO to form ester linkage. The --NH_2 tail on the gelatin was protonated in acidic solution during the synthesis, consequently transformed the hybrid gelatin-P123 to anionic surfactant with positive charges on the gelatin backbone. The positive charged of gelatin was suggested to promote the elongation of the micellar structures^{11,30,31,34}. Apart from that, the swelling effect of gelatin in water which enhanced at a higher gelatin concentration³⁵ expanding the spacing between SiO_4^- containing micelles, consequently increased the size of silica. Decomposition of gelatin and P123 molecules at high calcination temperature, produced a well-defined mesopores. The strong interaction between silicate-gelatin-P123 networks produced a stable composite, therefore calcination at high temperatures maintained the parallel pore network resulting in the pore expansion on silica^{30,36}.

SEM analysis. Figure 2 showed the SEM analysis of silica obtained using P123 (NS) and double template of P123-gelatin (NSG) at different weight ratios. In general, all silica samples showed the formation of elongated cube-like structure with the size increased at higher gelatin weight. Silica synthesized using P123 as template showed the formation of relatively small structure with the average particle size was estimated within $4\text{--}5\text{ }\mu\text{m}$. Following the addition of 1% of gelatin during the synthesis, there is a no significant differences on the morphology, but the particle sizes were slightly increased. When the silica was synthesized using a higher concentration of gelatin at 2% and 4%, a larger elongated cube-like particles were produced with the average sizes were determined at $6\text{--}9\text{ }\mu\text{m}$. The morphology analysis using SEM revealed that the addition of gelatin in the synthesis mixture managed to maintain the regularity of the three dimensional morphologies of the silica. However, the increase of gelatin concentration shifted the particles size distribution from 4 to $9\text{ }\mu\text{m}$. The histogram of particle size distribution, determine based on the length of the elongated cube revealed the enlargement of particles size with increasing the amount of gelatin in the reaction mixtures.

TEM analysis. TEM analysis of mesoporous silica produced using P123 and mesoporous silica from the mixture of P123 and 1% gelatin were carried out to provide high resolution morphology analysis. Figure 3a–c showed the TEM analysis of mesoporous silica produced using P123 without the presence of gelatin at different magnification. Although SEM analysis indicated the size of mesoporous silica was determined at $\sim 4\text{--}5$

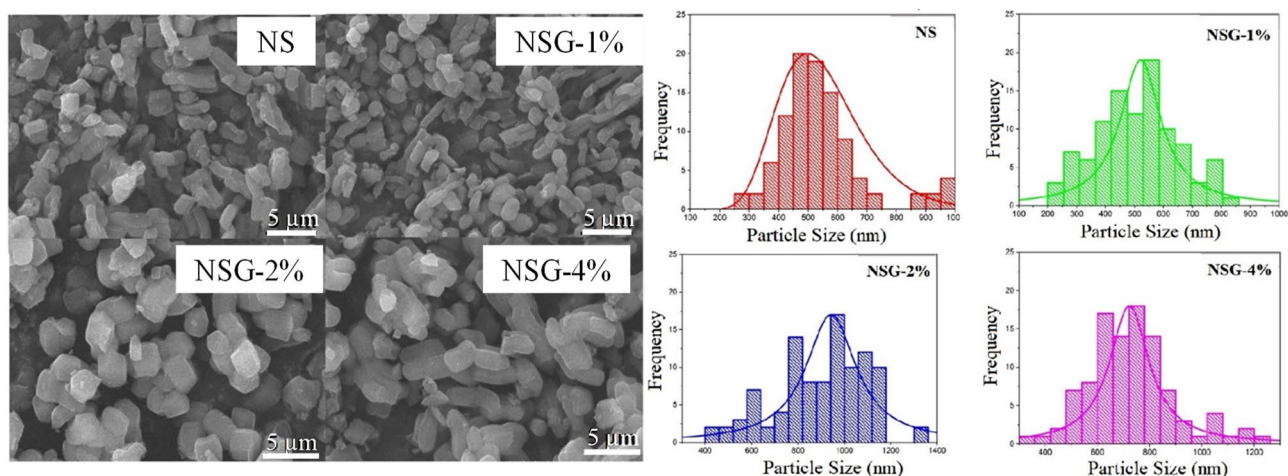


Figure 2. SEM analysis and the particle size distribution histogram of samples.

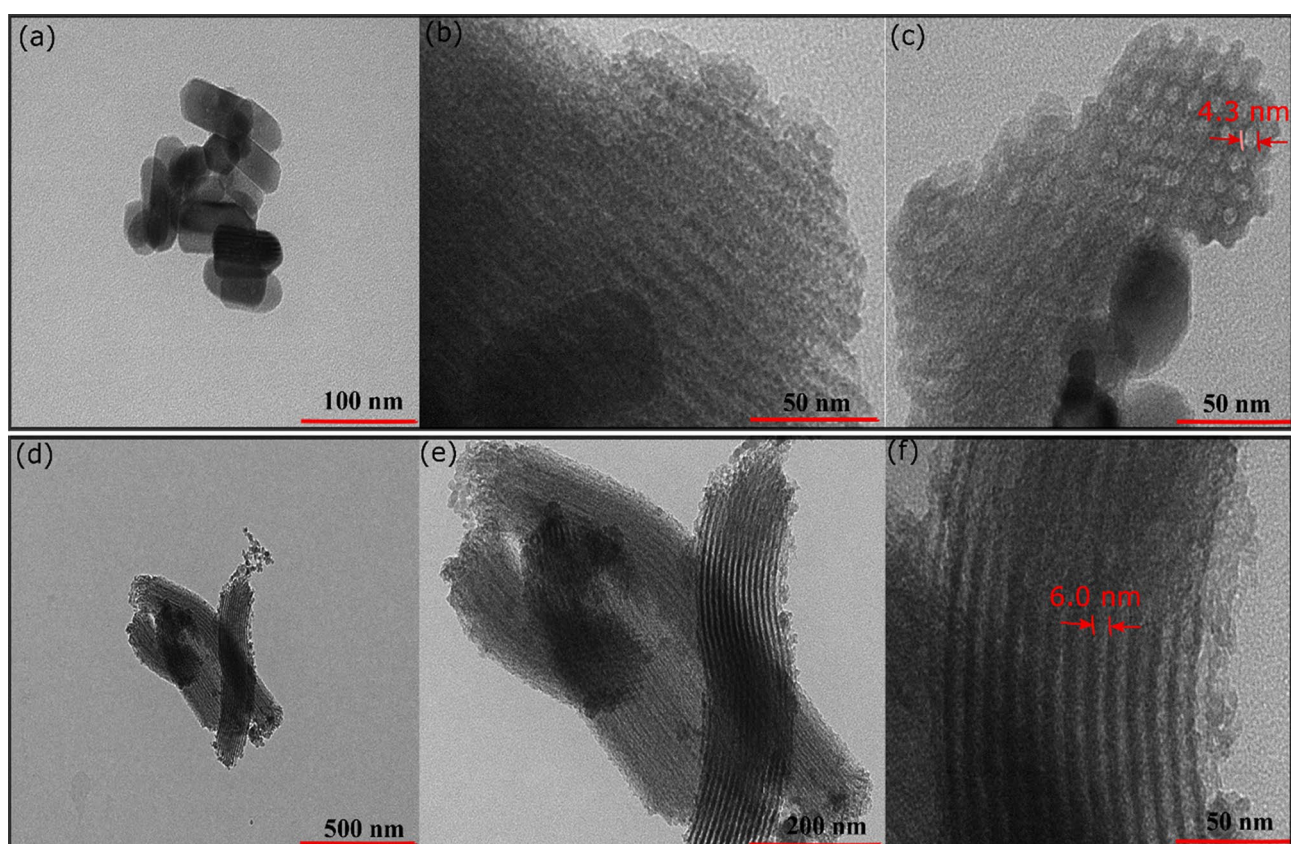


Figure 3. TEM analysis of NS (a–c) and NSG-1% (d–f).

um, the TEM analysis also revealed the formation of silica nanoparticles at ~100 nm size with a well-defined morphology (Fig. 3a). At much higher resolution, the presence of mesoporous channels was observed mainly on a larger silica particle (Fig. 3b). TEM analysis also revealed the average diameter of mesopores at ~4.3 nm (Fig. 3c). Mesoporous silica obtained using 1% gelatin and P123 mixture showed the formation of a well-defined mesoporous channel on each particle. The presence of gelatin produced mesoporous silica with larger particles size. The mesoporous channels were parallel and closely packed together forming a honeycomb structure with estimated diameter of 6.0 nm (Fig. 3d–f).

N₂ adsorption–desorption analysis. The N₂ adsorption–desorption isotherm and the pore size distribution of mesoporous silica was depicted in Fig. 4a,b. The isotherm plot (Fig. 4a) revealed the type IV features which ascribed to the formation of mesoporous material. The presence of hysteresis loop at P/P₀ 0.4–0.8 indicating a low level of regularity in the structure^{29,37}. The surface area of mesoporous silica produced using P123

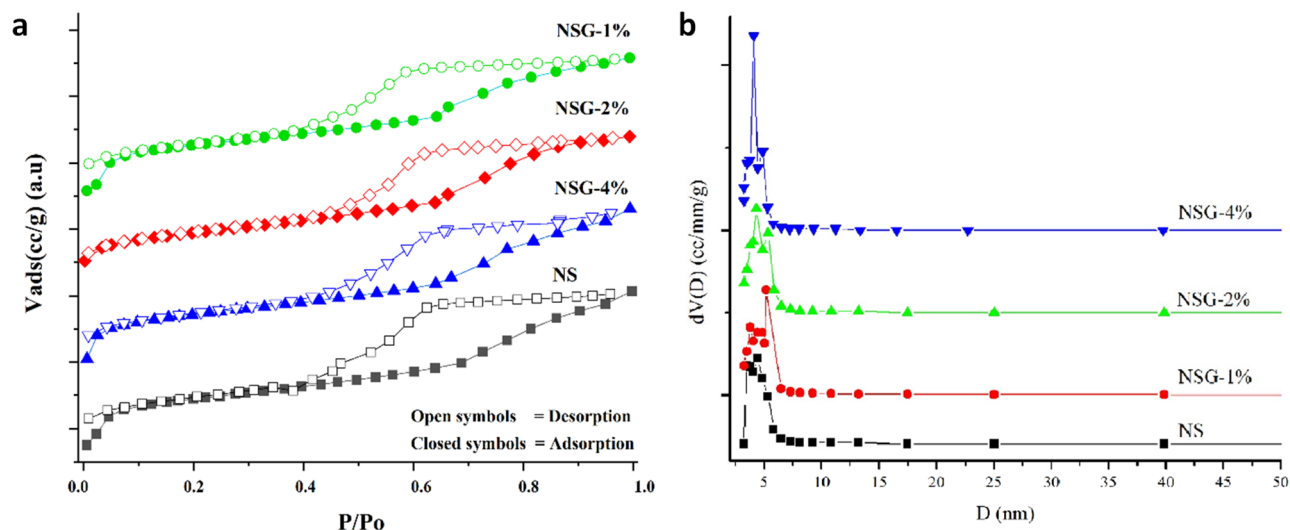


Figure 4. N_2 adsorption–desorption isotherm (a) and Pore size distribution (b) of samples.

Sample	S_{BET} (m^2/g) ^a	S_{micro} (m^2/g) ^b	V_{total} (cc/g)	V_{micro} (cc/g) ^b	V_{meso} (cc/g) ^c	D (nm) ^c
NS	484.05	75.08	0.599	0.062	0.537	6.66
NSG-1%	528.82	50.23	0.685	0.034	0.646	7.14
NSG-2%	512.21	52.38	0.676	0.038	0.638	7.14
NSG-4%	479.10	31.04	0.626	0.033	0.593	6.55

Table 2. Textural properties of samples. ^a S_{BET} (surface area) by BET method, measured at $P/P_0 < 0.3$ ^b S_{micro} and V_{micro} by t-plot method. ^c S_{meso} and D_{meso} by DFT method.

was determined at $484.05 \text{ m}^2/\text{g}$. The presence of gelatin significantly enhanced the surface area of mesoporous silica to $528.82 \text{ m}^2/\text{g}$ at 1% gelatin concentration. The pore volume was also improved to 0.646 cc/g compared to only 0.537 cc/g for P123 silica (Table 2). Further increased of gelatin loading to 2% and 4% slightly reduced the surface area and the pore volume, however the values were still higher than silica without gelatin. The pore size distribution of mesoporous silica obtained using P123 showed a wide pore size distribution within 2–20 nm of diameter (Fig. 4b). There is an apparent enlargement of pore diameter from 2–10 nm on to 2–14 nm with introduction of gelatin in the synthesis mixtures. Figure 4b also showed a nearly identical wide bimodal pore size distribution with two clearly peaks for all the samples. For each radius size, the increased of nitrogen uptake was observed as the concentration of gelatin increased. The observation implied the role of gelatin to increase the pore size and pore volume of mesoporous silica. It is estimated that with only 1% addition of gelatin in the synthesis mixture, contributed to the expansion of pore diameter by $\sim 1\text{--}2 \text{ nm}$. The same phenomenon was also reported by previous researchers while using trimethylbenzene as pore expander in the synthesis of mesoporous silica nanoparticles³⁶.

FTIR analysis. The functional group of mesoporous silica was determined using FTIR analysis shown in Fig. 5. All samples showed absorption bands at 1075 cm^{-1} , 981 cm^{-1} , 802 cm^{-1} and 484 cm^{-1} which corresponded to Si–O–Si symmetric stretching vibration, stretching Si–OH, network SiO₂ and Si–O–Si bending, respectively. Si–O–Si symmetric stretching vibrations at 1075 cm^{-1} showed the reduction of intensity following the use of high percentage of gelatin. The reduction of peak intensity indicated the decrease of regularity in silica crystalline framework^{18,34,38}. This observation is accompanied with the reduction of network SiO₂ band at 802 cm^{-1} . Meanwhile, the Si–OH peak at 981 cm^{-1} showed the increased of intensity in silica synthesized using 1% and 2% of gelatin concentration. The emergence of Si–OH suggested the strong interaction of gelatin with Si precursors in water, creating the swelling effect which is responsible for the expansion of mesopore. TEOS is spontaneously precipitated when dispersed in water to form silica particles. The presence of gelatin allowed the formation of Si–O–Si sol stabilized by P123–gelatin hybrid. The gel is predominantly contained the Si–O–Si network^{30,31,39}. Calcination at $500 \text{ }^\circ\text{C}$ removed the P123–gelatin templates, thus leaving the Si–O dangling bond to be compensated with trapped water from the gel swelling, generated terminal Si–OH bond. The results observed from FTIR analysis is crucial to provide information on the role of gelatin as spacer in reducing the growth of Si–O–Si bond network.

XRD analysis. Figure 6a showed X-ray diffractogram of silica obtained from P123 and a mixture of P123 and gelatin. All the silica samples showed similar diffractogram pattern with a broad peak centred at $2\theta = 22.9^\circ$

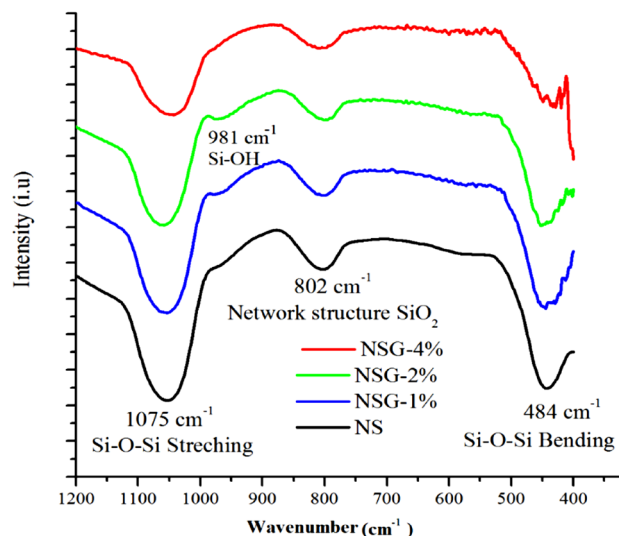


Figure 5. FTIR analysis of samples.

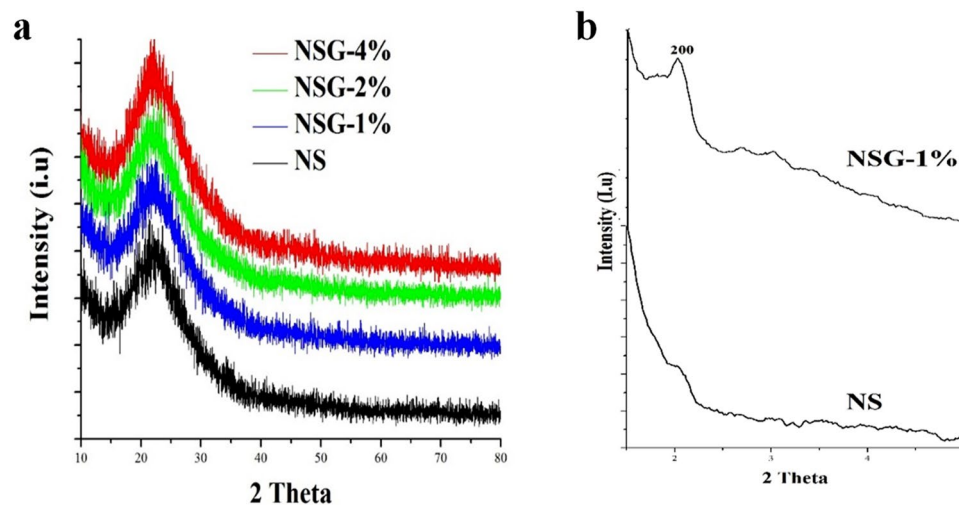


Figure 6. XRD analysis of mesoporous silica in wide (a) and low diffraction (b) angles.

which is a typical characteristic of amorphous silica^{1,37}. The intensity and the broadening of the peaks were slightly varied suggested the changes of structural properties and the crystallinity of the silica. Mesoporous silica with a lower concentration of gelatin showed a lower peak intensity as the result of smaller particle sizes. The crystalline structure of silica from P123 and a mixture of P123 and 1% gelatin were further analysed using a small angle XRD analysis in the 2-theta range of 0.5°–6° (Fig. 6b). Both silica samples showed the peak at 2.02° indexed as (200) plane, which is the characteristic of the two-dimensional hexagonal space group *p6mm*. However, the intensity of (200) plane of mesoporous silica from P123 and gelatin mixture was significantly higher than P123-derived silica. The results further confirmed the role of gelatin to increase the formation of mesopores in silica.

Adsorption of methylene blue. Figure 7a showed the performance of silica as adsorbent for methylene blue removal. The adsorption results were displayed as the effect of contact time on the adsorption capacity and the removal efficiency. The adsorption capacity of the silica samples when obtained at various gelatin concentration were ranged from 130 to 170 mg/g. The adsorption plot versus contact times showed the sharp increase of MB adsorption in the first 50 min before reaching equilibrium. Silica produced in the absence of gelatin only showed 78 mg/g of MB adsorption capacity, meanwhile the addition of gelatin significantly enhanced the adsorption capacity to 170 mg/g. Figure 7b showed the percentage of removal increased from 67 to 84% on the silica with increasing the gelatin concentration. The increase in the amount of methylene blue adsorption on silica produced with increasing gelatin concentration indicated that the enlargement of pore diameter is beneficial to increase MB diffusion and adsorption. Physical adsorption of MB on silica is enhanced by the high external surface area and the large mesopore diameter. Apart from that, the presence of functional group

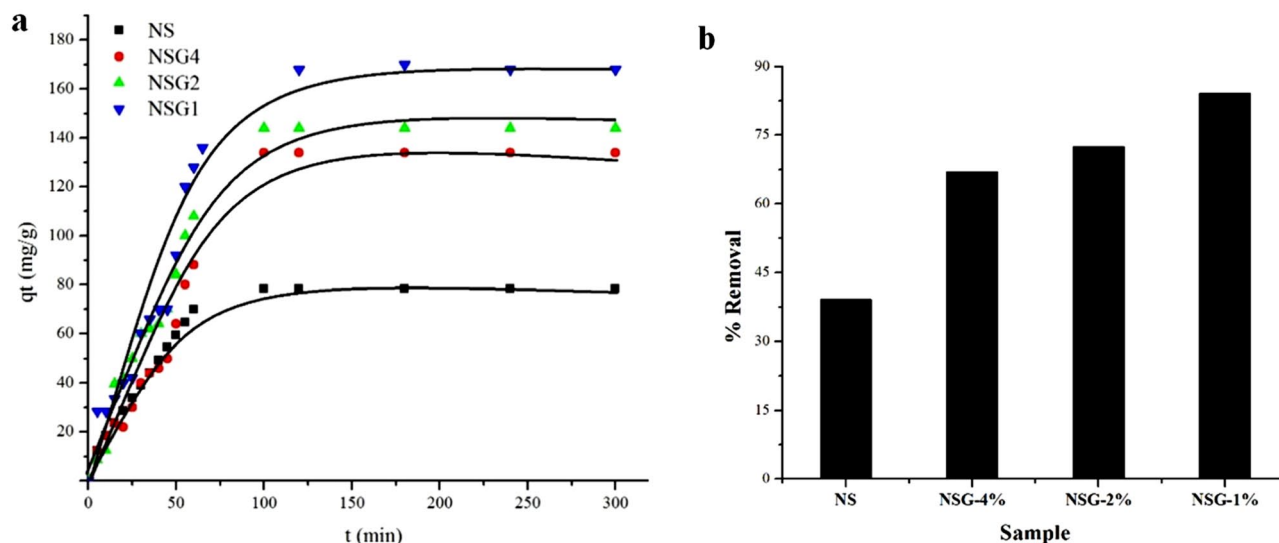


Figure 7. Adsorption capacity (a) and removal efficiency (b) of MB at initial concentration of 50 mg/L while using 50 mg of samples.

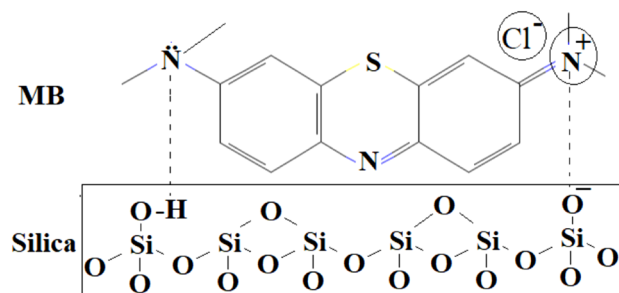


Figure 8. Scheme of interaction between MB and samples during adsorption.

increased the adsorption of MB via chemical interaction. Silanol functional group (Si–OH) interacted with MB via the lone pair of electrons in the nitrogen atom. The interaction between methylene blue and silica NSG is described in Fig. 8. It is suggested that there are two possible interactions that occur during the adsorption of methylene blue on silica. The first possibility is the electrostatic interaction between NH_2^+ on methylene blue as a cationic adsorbate molecule with O^{2-} on SiO_2 adsorbent. The second interaction occurs through hydrogen bonding between the amine groups on methylene blue with Si–OH on the silica surface. Similar mechanism on the interaction of silica and methylene blue have been proposed in several studies^{10,12,40}.

Based on Fig. 9a,b and Table 3, the pseudo-first-order linear plot shows a higher linearity with R^2 values of 0.93 compared to the pseudo-second order plot. The adsorption kinetic of methylene blue on silica is in accordance with the pseudo-first-order kinetics model. The first-order pseudo adsorption kinetics means that the adsorption capacity at equilibrium is directly be the main parameter for irreversible adsorption³². The concentration of adsorbate is considered to have no effect on the rate of adsorption and desorption so that when the active site of the adsorbent is covered by adsorbate, the adsorption rate only depends on the difference between the adsorption capacity at equilibrium with the adsorption capacity or formulated by $q_e - q_t$.

The effect of initial methylene blue concentration on the adsorption onto 50 mg NSG is shown in Fig. 10a. The equilibrium adsorption of methylene blue (Fig. 10b) increased from 35.29 to 177.06 mg/g with the increase of MB concentrations. A high concentration of MB enhanced the diffusion and the mass transfer due to the concentration gradient that was developed between the bulk solution and the surface of adsorbent⁴¹. The relatively large surface area from its tubular and bimodal pore structures, as well as the presence of microporous pore walls were responsible to provide adsorption sites for a highly concentrated methylene blue solution⁴². The presence of gelatin is responsible to determine the pore characteristic and specific surface area of NSG, which in turn promotes the adsorption capacity for organic waste removal^{6,43}. The equilibrium experimental adsorption data were fitted by the Langmuir and the Freundlich adsorption isotherms models to describe the mechanism of methylene blue adsorption onto mesoporous silica (Table 4). The Langmuir plot ($\frac{C_e}{q_e}$ versus C_e) for the adsorption data of methylene blue onto mesoporous silica fitted by a linear regression analysis (Fig. 10c). The Langmuir isotherm shows a good fit to the adsorption data with the regression coefficients (R^2) of 0.990. The data also fitted to the Freundlich plot, with the regression coefficients (R^2) was determined at 0.819. The

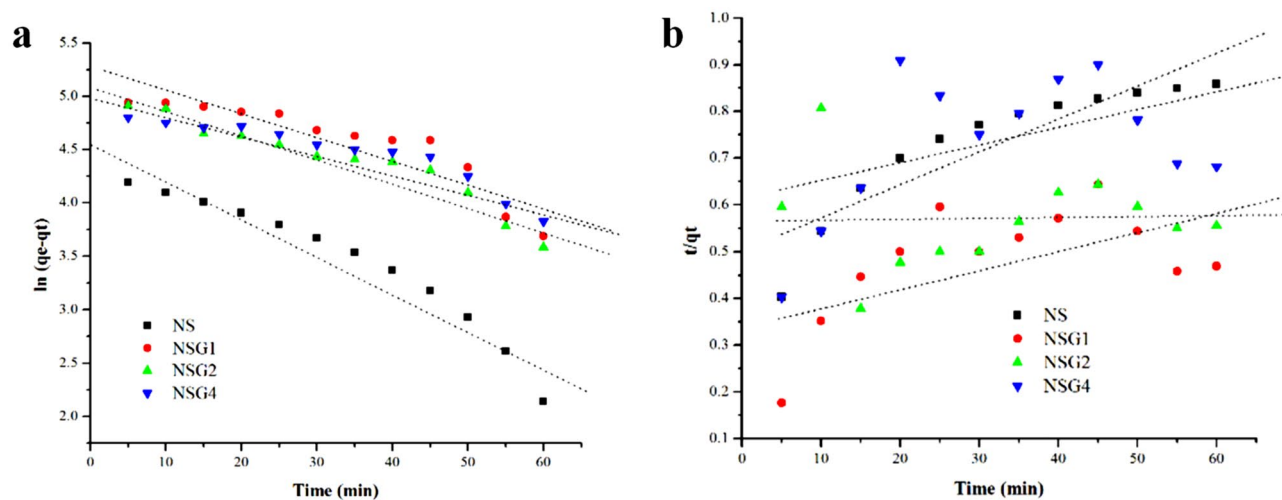


Figure 9. Pseudo-first (a) and pseudo-second-order (b) linear plots for the removal of MB by samples.

Sampel	Pseudo first order			Pseudo second order			
	R ²	k ₁ (min ⁻¹)	q _{cal} (mg/g)	R ²	k ₂ (min ⁻¹)	q _{cal} (mg/g)	q _e (mg/g)
NS	0.927	0.034	94.9	0.819	0.5023	1.99	78.36
NSG-1%	0.813	0.021	188.65	0.322	0.356	2.81	168.1
NSG-2%	0.916	0.021	159.6	0.003	0.564	1.77	144.0
NSG-4%	0.872	0.016	146.3	0.208	0.678	1.47	134.0

Table 3. Kinetic analysis of MB adsorption using samples.

values of q_{\max} and k were obtained from the slope and the intercept of the linear plots. The maximum adsorption capacity (q_{\max}) for NSG mesoporous silica was found determined at to be 200 mg/g which may be related to the presence of more mesopores in the structure of NSG. It is known that in mesopores the dispersive forces govern the amount adsorbed due to the increased adsorption potential due to the large pore size which accessible of methylene blue molecule¹². The results suggest that in the case of NSG mesoporous silica with its mesoporous pore wall structure⁴⁰ the amount adsorbed is governed, at least to some extent, by the mesopores, where dispersive interactions are predominant. The Freundlich isotherm (Fig. 10d) is represented by an empirical model that describes heterogeneous adsorption and assumes that the adsorption energy decreases exponentially with surface coverage. This Freundlich afforded a lower regression coefficient than Langmuir isotherm for mesoporous silica which indicates that the Langmuir isotherm model provides the most satisfactory fit to the experimental data.

Figure 11 shows that when the amount of adsorbent was increased from 5 to 70 mg, the percentage of removal was significantly enhanced to reach 94% removal. However, Table 5 indicates that the adsorption capacity is actually reduced from 330 mg/g to only 135 mg/g when using a high amount of adsorbent. The variation of adsorption capacity at different MB concentration and adsorbent amount was associated with the efficiency of mesoporous silica in absorbing methylene blue molecules. The low initial concentration allows MB molecules to enter the pores through electrostatic and chemical interactions. The reduction of removal efficiency with increasing the initial concentration was due to the saturation of MB molecules on the pore opening that were bonded to the available hydroxyl groups. This results in the formation of multi-layer MB or pore blockage during the adsorption process^{10,40}. At the beginning of adsorption until the equilibrium is reached, methylene blue will enter the pores and interact with the functional groups on the surface of silica. However, it is difficult to maintain the stability when the adsorbent amount is increased because the surface area and the pore volume were generally enhanced. Some of the pores will be occupied with MB at equilibrium, but the remaining empty sites will allow the MB molecules to desorb and diffused into the empty pores, regardless of the interaction with functional groups. This reversible adsorption process can be overcome by using the optimised adsorbent weight during adsorption. This result is in line with the previous studies which revealed that the increased weight of the adsorbent reduced the adsorption capacity, but enhanced percentage of removal especially in the high adsorbent dosage (> 20 mg)^{44,45}. Although the increasing weight of adsorbent reduced the adsorption capacity, in general the efficiency reached up to 94% removal when using a high amount of silica adsorbent. The results indicate the methylene blue is efficiently removed from water in the presence of more available adsorption sites.

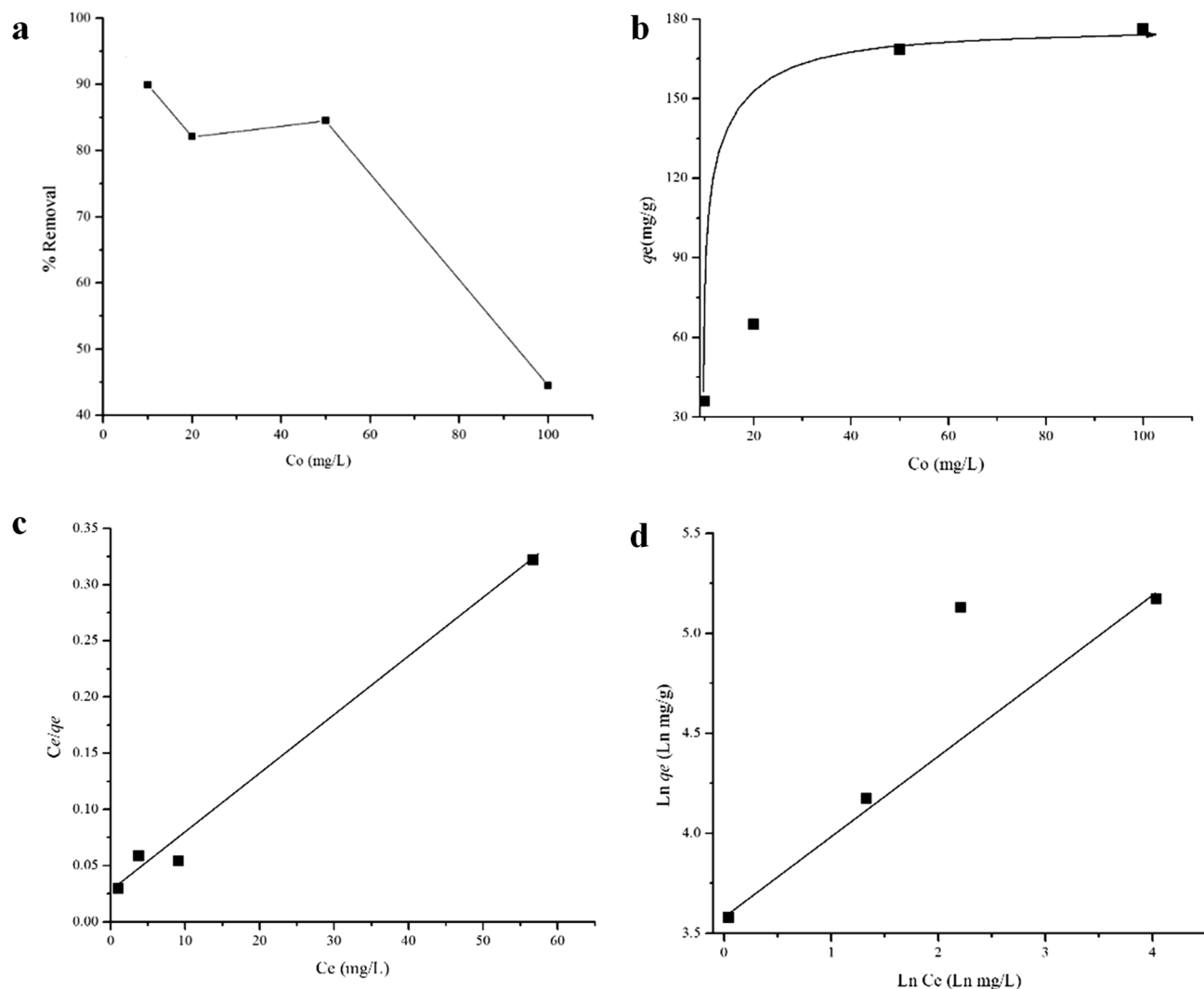


Figure 10. Initial concentration (C_o) effect (a), %Removal (b), Adsorption capacity at equilibrium (q_e) of MB fitted to isotherm of Langmuir (c) and Freundlich (d) Model.

Model	Formula	K	Note	R ²
Langmuir	$q_e = q_{max} \frac{C_e K_L}{1 + C_e K_L}$ or $\frac{C_e}{q_e} = \frac{1}{q_e K_L} + \frac{C_e}{q_{max}}$	0.2174 g/mg	$q_{max} = 200$ mg/g	0.999
Freundlich	$\ln q_e = \ln K_f + \frac{1}{n} \ln C_e$	1.312 (mg/g) (g/mg) ^{1/n}	$n = 10.4$	0.819

Table 4. Summary of experimental adsorption data fitted to the Langmuir and the Freundlich isotherm models.

Conclusion

Mesoporous silica synthesized in the presence of P123 and gelatin as green template showed the enlargement of mesopore diameter and particle size. Gelatin interacted with P123 to form extended amphoteric tail which facilitated the rearrangement of SiO_4^- during crystallisation process. As the results of increased surface area and pore diameter/volume, the silica showed a higher adsorption capacity to reach 168 mg/g at the equilibrium. There is also a possibility that a higher concentration of silanol group on silica obtained using gelatin-P123 hybrid template enhanced the adsorption of methylene blue with silica via chemical interaction.

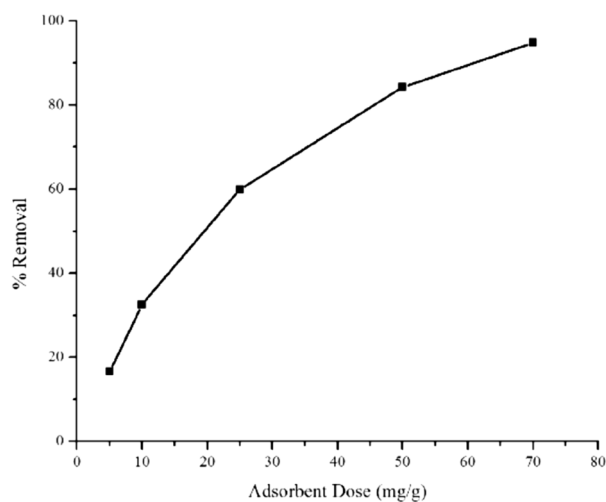


Figure 11. Adsorbent dose effect on %Removal of MB by NSG.

Adsorbent dose (mg)	q_{max} (mg/g)	Initial concentration (mg/L)	q_c (mg/g)
5	330.98	10	35.00
10	325.61	20	65.00
25	239.45	50	168.45
50	168.49	100	177.00
70	135.45	125	181.00

Table 5. The summary of adsorption capacity at variation of silica NSG adsorbent dosage and initial concentration of MB.

Data availability

The datasets used and analysed during the current study are available from the corresponding author on reasonable request.

Received: 9 May 2022; Accepted: 31 August 2022

Published online: 10 September 2022

References

- Chandrasekar, G., Son, W. J. & Ahn, W. S. Synthesis of mesoporous materials SBA-15 and CMK-3 from fly ash and their application for CO₂ adsorption. *J. Porous Mater.* **16**, 545–551 (2009).
- Albayati, T. M., Salih, I. K. & Alazzawi, H. F. Synthesis and characterization of a modified surface of SBA-15 mesoporous silica for a chloramphenicol drug delivery system. *Heliyon* **5**, e02539 (2019).
- Inagaki, S., Yokoo, Y., Miki, T. & Kubota, Y. Improvement of electric double-layer capacitance of ordered mesoporous carbon CMK-3 by partial graphitization using metal oxide catalysts. *Microporous Mesoporous Mater.* **179**, 136–143 (2013).
- Qian, T. *et al.* Radial-like mesoporous silica sphere: A promising new candidate of supporting material for storage of low-, middle-, and high- temperature heat. *Energy* **112**, 1074–1083 (2016).
- Zeng, S., Wang, R., Zhang, Z. & Qiu, S. Solventless green synthesis of sodalite zeolite using diatomite as silica source by a microwave heating technique. *INOCH* **70**, 168–171 (2016).
- Ulfa, M., Prasetyoko, D., Bahruji, H. & Nugraha, R. E. Green synthesis of hexagonal hematite (α -Fe₂O₃) flakes using pluronic F127-gelatin template for adsorption and photodegradation of ibuprofen. *Materials* **14**, 6779 (2021).
- Imoisili, P. E., Ukoba, K. O. & Jen, T. C. Green technology extraction and characterisation of silica nanoparticles from palm kernel shell ash via sol-gel. *J. Mater. Res. Technol.* **9**, 307–313 (2020).
- Reino Olegário da Silva, D. A., Bosmuler Zuge, L. C. & de Paula Scheer, A. Preparation and characterization of a novel green silica/PVA membrane for water desalination by pervaporation. *Sep. Purif. Technol.* **247**, 116852 (2020).
- Veisi, H., Tamoradi, T., Karmakar, B. & Hemmati, S. Green tea extract-modified silica gel decorated with palladium nanoparticles as a heterogeneous and recyclable nanocatalyst for Buchwald-Hartwig C-N cross-coupling reactions. *J. Phys. Chem. Solids* **138**, 109256 (2020).
- Wang, W. *et al.* All-into-one strategy to synthesize mesoporous hybrid silicate microspheres from naturally rich red palygorskite clay as high-efficient adsorbents. *Sci. Rep.* **6**, 1–14 (2016).
- Kéri, M. *et al.* Gelatin content governs hydration induced structural changes in silica-gelatin hybrid aerogels: Implications in drug delivery. *Acta Biomater.* **105**, 131–145 (2020).
- Zhou, C. *et al.* Preparation, characterization and adsorption evaluation of spherical mesoporous Al-MCM-41 from coal fly ash. *J. Taiwan Inst. Chem. Eng.* **52**, 147–157 (2015).
- Sachan, D., Ramesh, A. & Das, G. Green synthesis of silica nanoparticles from leaf biomass and its application to remove heavy metals from synthetic wastewater: A comparative analysis. *Environ. Nanotechnol. Monit. Manag.* **16**, 100467 (2021).

14. Imoisili, P. E., Ukoba, K. O. & Jen, T. Green technology extraction and characterisation of silica nanoparticles from palm kernel shell ash via sol–gel. *Integr. Med. Res.* **9**, 307–313 (2006).
15. Sapawe, N. *et al.* Synthesis of green silica from agricultural waste by sol-gel method. *Mater. Today Proc.* **5**, 21861–21866 (2018).
16. Okoronkwo, E., Imoisili, P. & Olisunle, S. O. Extraction and characterization of Amorphous Silica from Corn Cob Ash by Sol-Gel Method | Okoronkwo | Chemistry and Materials Research. *Chem. Mater. Res.* **3**, 68–72 (2013).
17. Lolage, M., Parida, P., Chaskar, M., Gupta, A. & Rautaray, D. Green Silica: Industrially scalable & sustainable approach towards achieving improved “nano filler–Elastomer” interaction and reinforcement in tire tread compounds. *Sustain. Mater. Technol.* **26**, e00232 (2020).
18. Liu, X. *et al.* A porous SiC/C composite material constructed by the ordered mesoporous SiC interfacing with the ordered mesoporous carbon and its supercapacitor performance. *J. Alloys Compd.* **881**, 160442 (2021).
19. Yu, Y. *et al.* Ionic liquid-Pluronic P123 mixed micelle stabilized water-soluble Ni nanoparticles for catalytic hydrogenation. *J. Colloid Interface Sci.* **415**, 117–126 (2014).
20. Wu, M. *et al.* Ordered mesoporous Zn-based supported sorbent synthesized by a new method for high-efficiency desulfurization of hot coal gas. *Chem. Eng. J.* **353**, 273–287 (2018).
21. Ulfa, M., Trisunaryanti, W., Falah, I. I. & Kartini, I. Synthesis of mesoporous carbon using gelatin as source of carbon by hard template technique and its characterizations. *IOSR J. Appl. Chem.* **4**, 1–7 (2014).
22. Petkova-olsson, Y., Oelschlaeger, C., Ullsten, H. & Järnström, L. Journal of colloid and interface science structural, microrheological and kinetic properties of a ternary silica-Pluronic F127-starch thermosensitive system. *J. Colloid Interface Sci.* **514**, 459–467 (2018).
23. Bernal, Y. P., Alvarado, J. & De Vasconcelos, E. A. Synthesis and characterization of carbon nanotubes / silica composites using gum Arabic. *Mater. Res. Express* <https://doi.org/10.1088/2053-1591/aacc3c> (2018).
24. Ulfa, M., Prasetyoko, D., Bahruji, H. & Nugraha, R. E. Green synthesis of hexagonal hematite (α -Fe₂O₃) flakes using pluronic F127-gelatin template for adsorption and photodegradation of ibuprofen. *Materials (Basel)*. **14**, 1–18 (2021).
25. Liang, F., Min, W., Hu, Y., Zilong, G. & Wensheng, Y. Efficient loading of curcumin into CTAB micelle-embedded silica particles for visualized pH detection. *Colloids Surf. A* **637**, 8 (2022).
26. Gisbert-González, J. M. *et al.* On the behavior of CTAB/CTAOH adayer on gold single crystal surface. *Electrochim. Acta* **391**, 138947 (2021).
27. Polikarpova, P., Akopyan, A., Shlenova, A. & Anisimov, A. New mesoporous catalysts with Brønsted acid sites for deep oxidative desulfurization of model fuels. *Catal. Commun.* **146**, 106123 (2020).
28. Wang, B., Dai, B., Kang, L. & Zhu, M. Synthesis of three-dimensional ordered mesoporous W-doped KIT-6 for oxidative desulfurization catalyst of fuels. *Fuel* **265**, 117029 (2020).
29. Vinu, A. *Mesoporous Non-Siliceous Materials and Their Functions. Advances in Nanoporous Materials* Vol. 1 (Elsevier, 2010).
30. Coradin, T., Bah, S. & Livage, J. Gelatine/silicate interactions: From nanoparticles to composite gels. *Colloids Surf. B* **35**, 53–58 (2004).
31. Sachithanadam, M. & Joshi, S. C. A new phenomenon of compressive strain recovery in gelatin-silica aerogel composites with sds. *Procedia Eng.* **75**, 51–55 (2014).
32. Ho, Y. S. Citation review of Lagergren kinetic rate equation on adsorption reactions. *Scientometrics* <https://doi.org/10.1023/B:SCIE.0000013305.99473.cf> (2004).
33. Alqadami, A. A., Naushad, M., Allothman, Z. A., Alsuhybani, M. & Algamdi, M. Excellent adsorptive performance of a new nanocomposite for removal of toxic Pb(II) from aqueous environment: Adsorption mechanism and modeling analysis. *J. Hazard. Mater.* **389**, 121896 (2020).
34. Lee, M. H. *et al.* Stability of boron-doped mesoporous SiC with high surface area in water-saturated air at 800 °C for diesel exhaust catalysis. *J. Solid State Chem.* **294**, 121905 (2021).
35. John Korthrop, R. H. & Kusitz, M. Swelling Bxd hydration of gelatixi. *J. Phys. Chem.* **35**, 162–184 (1930).
36. Turker, M. Z., Ma, K. & Wiesner, U. Bimodal morphology transition pathway in the synthesis of ultrasmall fluorescent mesoporous silica nanoparticles. *J. Phys. Chem. C* **123**, 9582–9589 (2019).
37. Palmqvist, A. E. C. Synthesis of ordered mesoporous materials using surfactant liquid crystals or micellar solutions. *Curr. Opin. Colloid Interface Sci.* **8**, 145–155 (2003).
38. Zhang, B., Huang, H., Zhao, B., Huang, J. & Li, W. Influence of mass ratios between SiC particles and chopped carbon fibers on properties of C/SiC/SiO₂ porous ceramics. *Ceram. Int.* **47**, 11574–11580 (2021).
39. Calabro, D. C., Valyocsik, E. W. & Ryan, F. X. In situ ATR/FTIR study of mesoporous silicate syntheses. *Microporous Mater.* **7**, 243–259 (1996).
40. Yuan, N., Cai, H., Liu, T., Huang, Q. & Zhang, X. Adsorptive removal of methylene blue from aqueous solution using coal fly ash-derived mesoporous silica material. *Adsorpt. Sci. Technol.* **37**, 333–348 (2019).
41. Anbia, M. & Karami, S. Desulfurization of gasoline using novel mesoporous carbon adsorbents. *J. Nanostruct. Chem.* **5**, 131–137. <https://doi.org/10.1007/s40097-014-0144-8> (2015).
42. Li, Z., Yan, W. & Dai, S. Surface functionalization of ordered mesoporous carbons a comparative study. *Langmuir* **21**, 11999–12006 (2005).
43. Ulfa, M., Prasetyoko, D., Mahadi, A. H. & Bahruji, H. Size tunable mesoporous carbon microspheres using Pluronic F127 and gelatin as co-template for removal of ibuprofen. *Sci. Total Environ.* **711**, 135066 (2020).
44. Kara, S., Aydinler, C., Demirbas, E., Kobya, M. & Dizge, N. Modeling the effects of adsorbent dose and particle size on the adsorption of reactive textile dyes by fly ash. *Desalination* **212**, 282–293 (2007).
45. Farzin Nejad, N., Shams, E., Amini, M. K. & Bennett, J. C. 239–246 Ordered mesoporous carbon CMK-5 as a potential sorbent for fuel desulfurization: Application to the removal of dibenzothiophene and comparison with CMK-3. *Microporous Mesoporous Mater.* <https://doi.org/10.1016/j.micromeso.2012.10.012> (2013).

Acknowledgements

Authors appreciate funding of Program Penelitian Kolaborasi Indonesia (PPKI) 2021 of Sebelas Maret University collaborated with Institut Teknologi Sepuluh November (ITS) and Gadjah Mada University (UGM) under project No. 102.1/UN27.22/HK.07.00/2021 for Maria Ulfa.

Author contributions

Conceptualization, M.U. and Z.A.F.; methodology, M.U.; software, M.U.; validation, M.U., H.B. and D.P.; formal analysis, M.U.; investigation, M.U.; resources, W.T.; data curation, M.U., Z.A.F., DP.; writing—original draft preparation, M.U.; writing—review and editing, M.U., H.B., N.A.S. and D.P.; visualization, M.U. and N.A.S.; supervision, W.T., H.B., D.P.; project administration, M.U.; Z.A. F, funding acquisition, M.U.

Competing interests

The authors declare no competing interests.

Additional information

Correspondence and requests for materials should be addressed to M.U.

Reprints and permissions information is available at www.nature.com/reprints.

Publisher's note Springer Nature remains neutral with regard to jurisdictional claims in published maps and institutional affiliations.



Open Access This article is licensed under a Creative Commons Attribution 4.0 International License, which permits use, sharing, adaptation, distribution and reproduction in any medium or format, as long as you give appropriate credit to the original author(s) and the source, provide a link to the Creative Commons licence, and indicate if changes were made. The images or other third party material in this article are included in the article's Creative Commons licence, unless indicated otherwise in a credit line to the material. If material is not included in the article's Creative Commons licence and your intended use is not permitted by statutory regulation or exceeds the permitted use, you will need to obtain permission directly from the copyright holder. To view a copy of this licence, visit <http://creativecommons.org/licenses/by/4.0/>.

© The Author(s) 2022